

# Detuned and Chirped Pulse Can Make Robust Qubit Control

Hanlae Jo, Han-gyeol Lee, and Jaewook Ahn\*  
*Department of Physics, KAIST, Daejeon 305-701, Korea*

We propose and demonstrate the existence of robust qubit control solutions, which require only chirping and detuning of a single laser pulse to manipulate a two-level system. Our numerical study, along with a proof-of-principle experiment performed with femtosecond laser interaction on cold atomic qubits, shows that a qubit driven by an as-shaped pulse can evolve through a cusp on the Bloch sphere, suggesting the qubit dynamics to be of robust against power fluctuation, due to zero curvature of fidelity always occurring at the cusp. This solution is particularly simple and thus applicable to a wide range of potential applications.

PACS numbers: 32.80.Qk, 37.10.Jk, 42.50.Dv, 42.50.Ex

Quantum information technologies (QITs) are expected to play an important role in the 21st century [1–7]. In QITs, quantum state, in particular the phase of a superposition state, carries information, but the noise in a quantum state is different from, and apparently much more sensitive to the environment than, the classical noise. So, dealing with the fragile nature of the quantum state requires high-fidelity fault-tolerant controls [6–8]. Quantum error correction, for example, needs computational infidelity below one part per ten thousand [9]. It is necessary to develop robust quantum control methods that tolerate fluctuations coming not only from the environment but also from control parameters themselves.

When a two-level quantum system (hereafter referred to as a qubit system) is controlled with coherent radiation, control error occurs due to power fluctuation and frequency flickering. Here the frequency is relatively well stabilized in current laser and microwave technologies [10], therefore power fluctuation is often the primarily source of error. In recent years, many ideas, such as composite pulse sequences [11–13], pulse-shape programming [16, 17], and optimization processes [14, 15] have been proposed to achieve robust quantum controls; however, these require either a train of well phase-maintained pulses or a complicated pulse shape, and/or reverse engineering. Instead, as a simple and practical approach, we consider only chirping and detuning a single Gaussian pulse to achieve the robustness. As to be discussed in the rest of the paper, we find that (1) this simple pulse shape (of a chirped and detuned pulse) makes a ground-state qubit evolve to an arbitrary qubit state, and that (2) the resulting qubit evolution is robust against power fluctuation. With a numerical investigation of time-domain Schrödinger equation (TDSE) simulations and, as a proof-of-principle demonstration, a femtosecond laser-atom interaction experiment, we show the occurrence of a cusp in qubit dynamics which proves the existence of a robust control condition. The physics behind this robust control may be understood in the context of a dynamic balance between the competing effects of chirping and detuning on qubit evolution, where the former induces an adiabatic flipping operation and the latter a Rabi-like oscillatory

return.

The problem under consideration is the evolution of a two-level system driven by a chirped and detuned Gaussian pulse. The electric-field of the given pulse is defined in the frequency domain as

$$E(\omega) = E_0 \exp \left[ -\frac{(\omega - \omega_c)^2}{\Delta\omega^2} + i\frac{c_2}{2}(\omega - \omega_c)^2 \right], \quad (1)$$

where  $\omega_c$  is the center frequency of the pulse,  $\Delta\omega$  the frequency bandwidth, and  $c_2$  the frequency-domain chirp rate. The time-domain electric-field of this pulse is the Fourier transform of  $E(\omega) + E(-\omega)$ , given by  $E(t) = \frac{\mathcal{E}(t)}{2} \exp[-i(\omega_c t + \alpha t^2 + \phi)] + c.c.$ , where  $\mathcal{E}(t) = 2E_0\sqrt{\Delta\omega/\tau} \exp(-t^2/\tau^2)$  is the Gaussian envelope with  $\tau = \sqrt{4/\Delta\omega^2 + c_2^2\Delta\omega^2}$  and  $\alpha = c_2/(2c_2^2 + 8/\Delta\omega^4)$  the temporal chirp, and  $\phi = -\tan^{-1}(c_2\Delta\omega^2/2)/2$  is the time-independent phase from the chirp.

For a two-level system described by  $|\psi\rangle = a_0|0\rangle + a_1|1\rangle$  with two state vectors  $|0\rangle$  and  $|1\rangle$  (of energies 0 and  $\hbar\omega_0$ , respectively), Hamiltonian is given after the rotating frame transformation and the rotating wave approximation by

$$H(t) = \frac{\hbar}{2} \begin{pmatrix} 0 & \Omega(t)e^{-i\int \Delta(t)dt + i\phi} \\ \Omega(t)e^{i\int \Delta(t)dt - i\phi} & 0 \end{pmatrix}, \quad (2)$$

where  $\Delta(t) = \delta - 2\alpha t$  is the instantaneous detuning with static detuning  $\delta = \omega_0 - \omega_c$  and  $\Omega(t) = \mu\mathcal{E}(t)/\hbar$  is the Rabi frequency with transition dipole moment  $\mu$ .

Robustness of two-level system dynamics is the second-order derivative, or the negative curvature of the fidelity function with respect to the fluctuation, that can be quantified with a quantum geometric tensor (QGT) [18, 19]. In our case, we parameterize the power fluctuation with the fractional error defined by  $\gamma = \delta\Omega/\Omega$  in Rabi frequency. So, the fidelity is defined by  $\mathcal{F} = |\langle\psi(\Omega)|\psi(\Omega + \gamma\Omega)\rangle|$  and the QGT (the diagonal component) is given by

$$g = -\frac{\partial^2 \mathcal{F}(\gamma)}{\partial \gamma^2} \Big|_{\mathcal{F}'=0} = \text{Re}(\langle \frac{\partial \psi}{\partial \gamma} | \psi_{\perp} \rangle \langle \psi_{\perp} | \frac{\partial \psi}{\partial \gamma} \rangle), \quad (3)$$

where  $|\psi_\perp\rangle$  is the orthonormal state with respect to  $|\psi\rangle$ . For a fluctuating Hamiltonian  $H' = (1 + \gamma)H$ , the state vectors initially at  $|\psi(t = -\infty)\rangle = |0\rangle$  and  $|\psi(t = -\infty)_\perp\rangle = |1\rangle$  evolve with the time-evolution matrix given by  $U(t) \simeq U_0(t) - \frac{i}{\hbar} U_0(t) \int_{-\infty}^t \gamma V(t') dt'$ , where  $U_0$  is the time-evolution matrix for  $H$  and  $V(t) = U_0^\dagger H U_0$ . Therefore, the QGT in Eq. (3) is given by

$$g = \langle 0 | \left( -\frac{i}{\hbar} \int_{-\infty}^{\infty} V dt \right)^\dagger | 1 \rangle \langle 1 | \left( -\frac{i}{\hbar} \int_{-\infty}^{\infty} V dt \right) | 0 \rangle \quad (4)$$

up to the second order of the small fluctuation  $\gamma$ .

Figure 1 shows the numerical calculation of the robustness using the QGT  $g$  and the fidelity  $\mathcal{F}$  for the two-level system dynamics driven by detuned and chirped pulses. To make the comparison easier, we use three dimensionless parameters  $\Delta' = \delta/\Delta\omega$ ,  $c'_2 = c_2\Delta\omega^2$ , and  $\Theta = \int_{-\infty}^{\infty} \Omega(t) dt$  (the pulse-area after shaping) to rewrite the pulse in Eq. (1) as

$$E(\omega) = E_0 \exp \left[ -\left( \frac{\omega - \omega_0}{\Delta\omega} + \Delta' \right)^2 + i \frac{c'_2}{2} \left( \frac{\omega - \omega_0}{\Delta\omega} + \Delta' \right)^2 \right], \quad (5)$$

where the amplitude is given by  $E_0 = \frac{\hbar\Theta}{2\mu\sqrt{\pi}}(4 + c'_2)^{-1/4}$ . The QGT,  $g(\Theta, c'_2)$ , is plotted for  $\Delta' = 0.637$  in Fig. 1(a), showing optimal robustness ( $g \approx 0$ ). It occurs at point **B** or  $(\Theta, c'_2, \Delta') = (1.77\pi, 2.5, 0.637)$ , when the evolution is targeted to the excitation probability  $P_e = 0.5$ . Less robust pulses with a smaller or larger chirp are also shown in Fig. 1(a), respectively denoted by **A** and **C**, which have small but not nonzero QGTs ( $g_{\mathbf{A}} = 0.11$  and  $g_{\mathbf{C}} = 0.05$ ). (Note that the  $g = 0$  points for smaller or larger chirps may also be found at different  $\Delta'$ 's and  $\Theta$ 's.) Therefore, as shown in Fig. 1(b), the optimal robust pulse **B** exhibits a significantly flattened fidelity curve, or more robust evolution, than other pulses and the Rabi-type evolution to the same final population. In terms of the high-fidelity range of  $\gamma$ , for example, when the fidelity is larger than 0.999 the optimal pulse **B** shows 3.5 times wider range of robust evolution than the Rabi oscillation.

The horizontal line segment in Fig. 1 corresponds to a  $\Theta$ -trajectory on the Bloch sphere. Figure 2 shows such trajectories passing through respectively **A**, **B**, and **C** points, which are plotted as a function of  $\Theta$ , while  $c'_2$  and  $\Delta'$  are fixed in each trajectory. As clearly shown in Fig. 2(a), the trajectory shape changes, as  $c'_2$  increases, from a looped curve (case **A**) to an unlooped one (case **C**), and, as a result, a cusp is formed in-between (case **B**). The trajectory with a cusp is particularly interesting in topology, because the singular nature of the cusp allows both derivatives of any pair of mutually-orthogonal coordinates, on the Bloch sphere, with respect to  $\Theta$  are always zero [20], i.e.,  $\frac{d|\psi\rangle}{d\Theta} = \frac{\partial|\psi\rangle}{\partial\theta} \frac{d\theta}{d\Theta} + \frac{\partial|\psi\rangle}{\partial\phi} \frac{d\phi}{d\Theta} = 0$ , at the cusp point which is **B**. This occurrence ensures the QGT to be zero (the optimal robustness). At an even higher pulse area and different chirp rate, similarly an

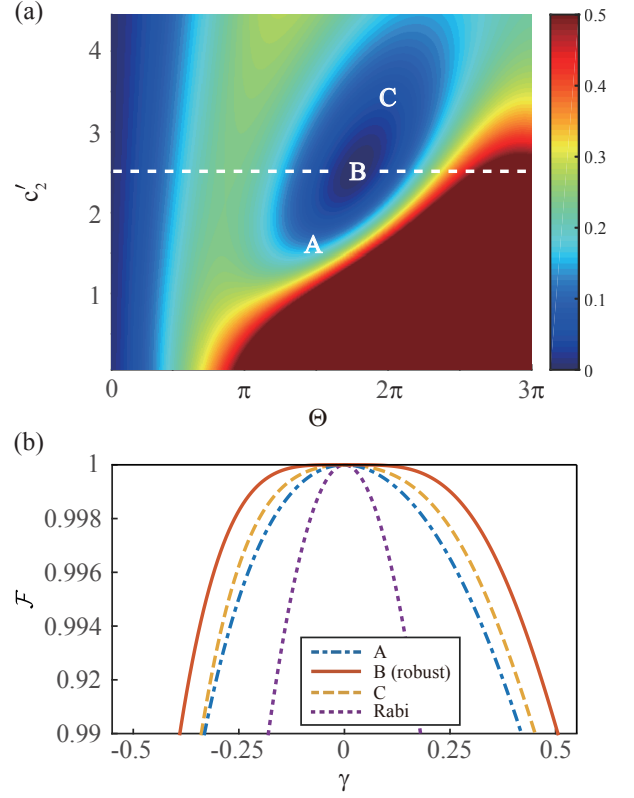


FIG. 1: (Color online) Robustness map  $g(\Theta, c'_2)$  at  $\Delta' = 0.637$  (see text for definition): The QGT  $g$  is plotted as a function of the pulse area  $\Theta$  and the chirp rate  $c'_2$ , at a fixed detuning  $\Delta' = 0.6372$ . The most robust point is located at **B**, giving  $g_{\mathbf{B}} < 1.128e - 6$  limited by our calculation accuracy, while  $g_{\mathbf{A}} = 0.11$ ,  $g_{\mathbf{C}} = 0.05$ , and  $g_{\text{Rabi}} = 0.62$ . (b) Fidelity curves  $\mathcal{F}(\gamma)$ : The fidelity curve (red solid line) is calculated at **B** as a function of the fluctuation  $\gamma$  (see text for definition) and compared with cases **A** and **C** (blue dash-dotted and yellow dashed lines, respectively) and also with the Rabi-type evolution (purple dotted line) to the same excited-state probability  $P_e = 0.5$  as the **B** case.

other cusp occur to make another robust point, and so on (not shown).

To verify the robust qubit operations experimentally, we performed femtosecond laser-atom interaction experiments. The experimental set-up and procedure are similar to those in our previous experimental work [21–24]. In brief, a magneto-optical trap (MOT) was used to confine rubidium atoms ( $^{85}\text{Rb}$ ) in a small volume for uniform laser interaction. The diameter of the atomic vapor inside the MOT was  $300 \mu\text{m}$ , about 43% of the laser diameter. The laser setup consisted of a femtosecond laser amplifier and, as a pulse-shaping device, an acousto-optic programmable dispersive filter (AOPDF) [25]. Femtosecond laser pulses were initially generated from a mode-locked titanium-sapphire laser oscillator and amplified up to 0.85 mJ of single-pulse energy at a repetition rate of 1 kHz. Each laser pulse was then shaped

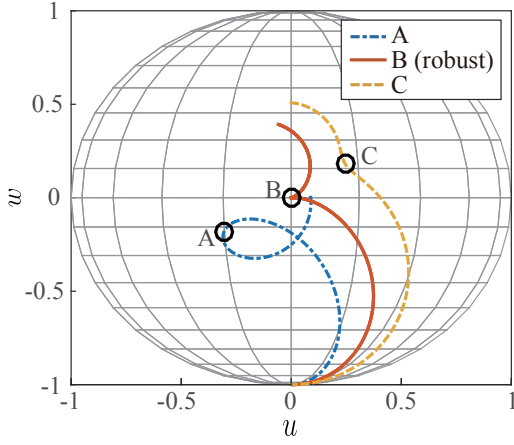


FIG. 2: (Color online)  $\Theta$ -parameterized trajectories on Bloch sphere: The final state  $|\psi(t = \infty)\rangle$  of a two-level system after a chirped- and detuned-pulse interaction is plotted with a Bloch vector. The trajectories through **A**, **B**, and **C** in Fig. 1 are plotted with blue dash-dotted, red solid, yellow dashed lines, respectively.

with four experimental parameters: center frequency, chirp rate, bandwidth, and pulse intensity. The first three were programmed with the AOPDF and the last, the laser intensity, was fine-controlled with a half-wave

plate sandwiched between a pair of cross-polarizers. The center wavelength of the laser pulse was tunable from  $\lambda_c = 792$  to  $802$  nm, which corresponded to the detuning range between  $\delta = -8.38 \times 10^{12}$  and  $2.13 \times 10^{13}$  rad/s. The laser bandwidth was fixed at  $\Delta\lambda_{\text{FWHM}} = 10.4$  nm ( $\Delta\omega_{\text{FWHM}} = 1.86 \times 10^{13}$  rad/s), and the frequency chirp rate  $c_2$  was changed from  $-40,000$  to  $40,000$   $\text{fs}^2$  for various experiments. The two-level system was formed with  $5S_{1/2}$  and  $5P_{1/2}$ , the ground and the first-excited states of atomic rubidium ( $^{85}\text{Rb}$ ). The population leakage to other states, including  $5P_{3/2}$ ,  $5D$ , and ionization levels, was less than 2% within the experimental parameter range. After the atoms were controlled by the as-shaped laser pulse, those in the excited state were ionized by a probe laser pulse, which was the frequency-doubled split-off from the unshaped laser pulse, and measured with a micro-channel plate detector. The total sequence of experiment was tuned at 2 Hz cycle to maintain the MOT density by using mechanical shutters for femtosecond laser pulses, and acousto-optic modulators for MOT lasers. The MOT lasers were turned off before the arrival of the control pulse to initialize the atomic state in the ground state and turned on after the interaction to restore the MOT.

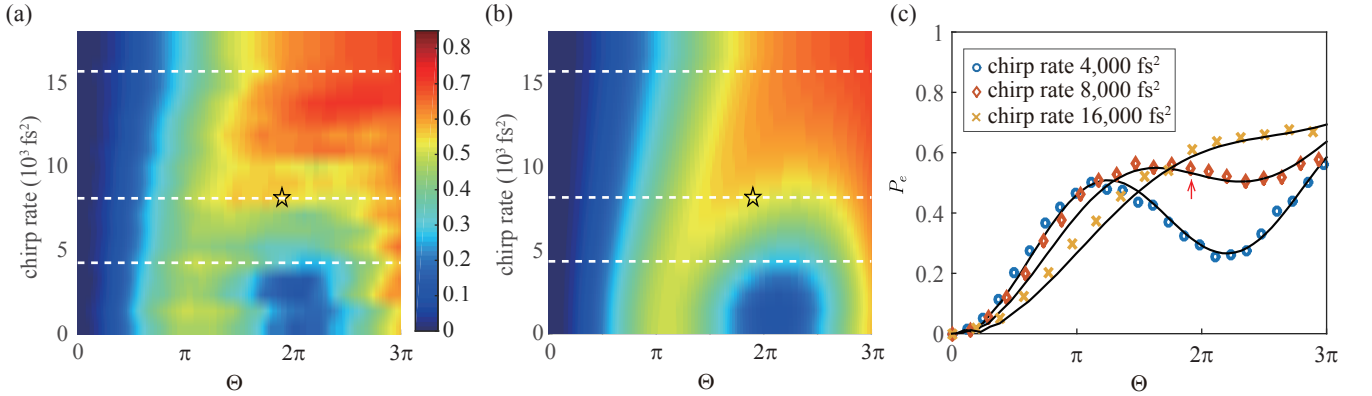


FIG. 3: (Color online) The probability  $P_e(\Theta, c_2)$  of the excited-state ( $5P_{1/2}$  of rubidium) after the detuned and chirped Gaussian pulse excitation as a function of the pulse-area  $\Theta$  and the chirp rate  $c_2$ , while the detuning and laser bandwidth are fixed at  $\delta = 3.5$  nm and  $\Delta\omega_{\text{FWHM}} = 3.1 \times 10^{13}$  rad/s, respectively. (a) Experimentally obtained probability map  $P_e^{\text{exp}}(\Theta, c_2)$ , to which the measured atom population was converted using Rabi-oscillation calibration measurements (see text for detail). (b) Theoretical result  $P_e^{\text{TDSE}}(\Theta, c_2)$ , obtained using the TDSE calculation for an atom cloud of a Gaussian profile with a diameter 47% of the Gaussian laser beam diameter. (c) The behavior of the population  $P_e(\Theta)$ s for selected chirp rates  $c_2 = 4,000$  (blue circles),  $8,000$  (red diamonds), and  $16,000$   $\text{fs}^2$  (yellow crosses), respectively shows good agreement with the theoretical lines. The star and arrow symbols represent the robust condition.

Experimental results are compared with numerical calculation in Fig. 3. The excitation probability  $P_e(\Theta, c_2)$  of atoms after as-shaped laser pulses was probed as a

function of the pulse-area  $\Theta$  and the chirp rate  $c_2$ , while the detuning was fixed at  $\delta = 3.5$  nm ( $\Delta' = 0.56$ ). The results are shown in Fig. 3(a). We note that, to retrieve

$P_e^{\text{exp}}(\Theta, c_2)$  from the measured counts of the ionized electrons, we used Rabi-oscillation calibration method [22]. In addition, we assumed the minor discrepancy at the high laser-power region ( $\Theta > 2.5\pi$ ) was attributed to the effect of a possible pre-pulse with 0.4% energy and small relative phase. The result of TDSE simulation for the given qubit dynamics is shown in Fig. 3(b), where the spatial inhomogeneity [22] of the laser-atom interaction is taken into account. The spatial inhomogeneity is parametrized with the size ratio between the laser beam and the atomic cloud, where the latter is characterized by the convolution with the probing ionization beam. The ideal robust control point, marked with star in the figures is located at  $(\Theta, c_2', \Delta') = (1.9\pi, 2.79, 0.56)$  or  $(\Theta, c_2, \Delta) = (1.9\pi, 8.1 \times 10^3 \text{ fs}^2, 1.04 \times 10^{13} \text{ rad/s})$ . The overall behavior of the retrieved qubit dynamics, selectively compared in Fig. 3(c), exhibits good agreement.

We now turn our attention to generalization of our robust qubit control method to arbitrary target states. We experimentally probed the two-dimensional section at  $\Delta' = 0.56$  of the three-dimensional parameter space of  $(\Delta', c_2', \Theta)$  as illustrated in Fig. 4, where the tested robust point is marked with a star. Further numerical simulation finds that robust control conditions occur along a line (the solid line with circles). With the as-found robust-control conditions,  $\Theta$ -trajectories to various target probabilities are plotted on the Bloch sphere in the inset. As clearly shown in the figure, robust control can be made to arbitrary target probabilities and, by considering the azimuthal angle of the Bloch vector is easily set with the laser phase, our method can be generalized to any arbitrary target states on the Bloch sphere.

In summary, we have shown that detuned and chirped pulses can implement robust transfer of a ground-state qubit to an arbitrary state. Our numerical study finds that, with a proper combination of laser detuning and chirp rate, cusps can be formed in qubit evolution. As chirp rate increases, the trajectory on the Bloch sphere topologically changes from a loop-the-loop to an un-looped curve and the winding number changes from one to zero. Therefore, a cusp is always formed in-between, which suggests that the qubit dynamics becomes robust against power fluctuation. As a proof-of-principle experimental verification, we performed ultrafast optical manipulation of cold rubidium atoms, and the result agrees strongly with the numerical simulations. Our robust control solution is particularly simple, requiring only chirping and detuning of a Gaussian pulse. It is hoped that our method becomes useful in a wider range of applications.

The authors are grateful to Stéphane Guérin, C. H. Raymond Ooi, Yunheung Song, and Adam Massey for fruitful discussions. This research was supported by Samsung Science and Technology Foundation [SSTF-BA1301-12].

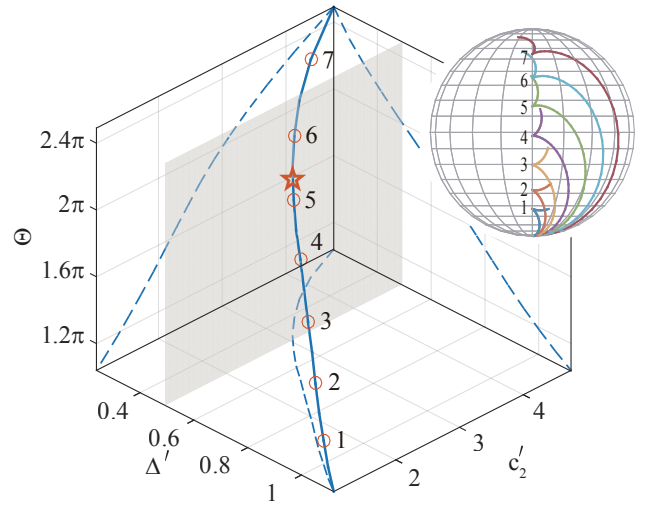


FIG. 4: (Color online) Robust control conditions in the parameter space  $(\Delta', c_2', \Theta)$ : Red circles represent the parameters for detuned and chirped pulses that induce robust qubit control to various target probabilities, and the solid and dashed lines are the numerical fit and its projections to each plane. The inset shows the  $\Theta$ -trajectories, on the Bloch sphere, each corresponding to a vertical line (with fixed  $c_2'$  and  $\Delta'$ ) through a numbered red circle and the robust control occurs at each cusp.

\* Electronic address: jwahn@kaist.ac.kr

- [1] C. H. Bennett, G. Brassard, C. Crépeau, R. Jozsa, A. Peres, and W. K. Wootters, Phys. Rev. Lett. **70**, 1895 (1993).
- [2] X. S. Ma *et al.*, Nature (London) **489**, 269 (2012).
- [3] M. Takamoto, F.-L. Hong, R. Higashi, and H. Katori, Nature (London) **435**, 321 (2005).
- [4] E. M. Kessler, P. Kómár, M. Bishof, L. Jiang, A. S. Sørensen, J. Ye, and M. D. Lukin, Phys. Rev. Lett. **112**, 190403 (2014).
- [5] D. Deutsch, Proc. R. Soc. London A **400**, 97 (1985).
- [6] J. Chiaverini *et al.*, Nature (London) **432**, 602 (2004).
- [7] J. Kelly *et al.*, Nature (London) **519**, 66 (2015).
- [8] P. W. Shor, Phys. Rev. A **52**, R2493 (1995).
- [9] E. Knill, Nature (London) **434**, 39 (2005).
- [10] S. A. Diddams, D. J. Jones, J. Ye, S. T. Cundiff, J. L. Hall, J. K. Ranka, R. S. Windeler, R. Holzwarth, T. Udem, and T. W. Hänsch, Phys. Rev. Lett. **84**, 5102 (2000).
- [11] M. H. Levitt, Prog. Nucl. Mag. Res. Spect. **18**, 61 (1986).
- [12] K. R. Brown, A. W. Harrow, and I. L. Chuang, Phys. Rev. A **70**, 052318 (2004).
- [13] B. T. Torosov, S. Guérin, and N. V. Vitanov, Phys. Rev. Lett. **106**, 233001 (2011).
- [14] N. Khaneja, T. Reiss, C. Kehlet, T. Schulte-Herbrüggen, and S. J. Glaser, J. Magn. Reson. **172**, 296 (2005).
- [15] R. L. Kosut, M. D. Grace, and C. Brif, Phys. Rev. A **88**, 052326 (2013).
- [16] D. Daems, A. Ruschhaupt, D. Sugny, and S. Guérin, Phys. Rev. Lett. **111**, 050404 (2013).

- [17] A. Ruschhaupt, X. Chen, D. Alonso, and J. G. Muga, New J. Phys. **14**, 093040 (2012).
- [18] J. P. Provost and G. Vallee, Commun. Math. Phys. **76**, 289 (1980).
- [19] R. Cheng, arXiv:1012.1337v2 (2013).
- [20] J. W. Bruce and P. Giblin, *Curves and Singularities* (Cambridge University Press, 1984).
- [21] J. Lim, H. Lee, S. Lee, C. Y. Park, and J. Ahn, Sci. Rep. **4**, 5867 (2014).
- [22] H. Lee, H. Kim, and J. Ahn, Opt. Lett. **40**, 510 (2015).
- [23] H. G. Lee, Y. Song, H. Kim, H. Jo, and J. Ahn, Phys. Rev. A **93**, 023423 (2016).
- [24] Y. Song, H. G. Lee, H. Jo, and J. Ahn, Phys. Rev. A **94**, 023412 (2016).
- [25] P. Tournois, Opt. Comm. **140**, 245 (1997).